Atmospheric Environment 45 (2011) 4060–4072

Contents lists available at ScienceDirect

Atmospheric Environment

journal homepage: www.elsevier.com/locate/atmosenv

Impact of fair-weather cumulus clouds and the Chesapeake Bay breeze on pollutant transport and transformation

Christopher P. Loughner [a,*], Dale J. Allen [a], Kenneth E. Pickering [b], Da-Lin Zhang [a], Yi-Xuan Shou [c], Russell R. Dickerson [a]

[a] Department of Atmospheric and Oceanic Science, University of Maryland, College Park, MD 20742, USA
[b] NASA Goddard Space Flight Center, Greenbelt, MD 20771, USA
[c] National Satellite Meteorological Center, China Meteorological Administration, Beijing 100081, PR China

ARTICLE INFO

Article history:
Received 9 December 2010
Received in revised form
31 March 2011
Accepted 1 April 2011

Keywords:
Community Multiscale Air Quality (CMAQ) model
Horizontal grid resolution
Fair-weather cumulus clouds
Sulfur dioxide
Bay breeze
Ozone

ABSTRACT

Two fine-scale meteorological processes, fair-weather cumulus cloud development and a bay breeze, are examined along with their impacts on air chemistry. The impact of model resolution on fair-weather cumulus cloud development, transport of pollutants through clouds, sulfur dioxide to sulfate conversion in clouds, and the development of the Chesapeake Bay breeze are examined via 13.5, 4.5, 1.5, and 0.5 km resolution simulations covering the Washington – Baltimore area. Results show that as the resolution increases, more pollutants are transported aloft through fair-weather cumulus clouds causing an increase in the rate of oxidation of sulfur dioxide to sulfate aerosols. The high resolution model runs more nearly match observations of a local pollutant maximum near the top of the boundary layer and produce an increase in boundary layer venting with subsequent pollutant export. The sensitivity of sulfur dioxide to sulfate conversion rates to cloud processing is examined by comparing sulfur dioxide and sulfate concentrations from simulations that use two different methods to diagnose clouds. For this particular event, a diagnostic method produces the most clouds and the most realistic cloud cover, has the highest oxidation rates, and generates sulfur dioxide and sulfate concentrations that agree best with observations. The differences between the simulations show the importance of accurately simulating clouds in sulfate simulations. The fidelity of the model's representation of the bay breeze is examined as a function of resolution. As the model resolution increases, a larger temperature gradient develops along the shoreline of the Chesapeake Bay causing the bay breeze to form sooner, push farther inland, and loft more pollutants upward. This stronger bay breeze results in low-level convergence, a buildup of near surface ozone over land and a decrease in the land-to-sea flux of ozone and ozone precursors as seen in measurements. The resulting 8 h maximum ozone concentration over the Bay is 10 ppbv lower in the 0.5 km simulation than in the 13.5 km simulation.

1. Introduction

Ozone and aerosols have health and climate implications. Ground-level ozone may cause permanent lung damage (Mudway and Kelly, 2000) and ground-level aerosols may produce heart and lung disease (Docker et al., 1993; Samet et al., 2000), and both tropospheric ozone and aerosols impact the radiative budget (Shine, 2000). The production of secondary pollutants, such as ozone and sulfate aerosols, depends on emissions, meteorological conditions, and the chemical composition of the atmosphere. Numerical Weather Prediction (NWP) and chemical models along with observations have been used to investigate how pollutants evolve in the atmosphere, to forecast air quality and climate impacts of pollutants, and to help evaluate air pollution and climate change mitigation plans.

Fine scale weather structures, such as fair-weather cumulus clouds and a sea breeze, influence air chemistry. Clouds play an important role in the sulfur cycle. While gas phase sulfur dioxide oxidation rates are slow, sulfur dioxide can be oxidized rapidly through heterogeneous reactions in clouds when ozone is present and the pH is greater than 5 or when hydrogen peroxide is present over all pH values (Daum, 1990; Finlayson-Pitts and Pitts, 2000; Jacob et al., 1989). For example, Eatough et al. (1984) studied the conversion of sulfur dioxide to sulfate aerosols in a power plant plume near the Pacific Ocean coast and found that on average

* Corresponding author. Tel.: +1 775 530 7555; fax: +1 301 314 9482.
E-mail address: loughner@atmos.umd.edu (C.P. Loughner).

1352-2310/$ – see front matter © 2011 Elsevier Ltd. All rights reserved.
doi:10.1016/j.atmosenv.2011.04.003

24–36% of the sulfur dioxide was oxidized in 1 h in the presence of fog, but only 2–4% of the sulfur dioxide was oxidized when the plume was not located in a cloud. The pH of rainwater reported by the National Atmospheric Deposition Program/National Trends Network in the Mid-Atlantic is around 4.5, so the quickest path of sulfur dioxide to sulfate conversion in the region is in the presence of liquid water and hydrogen peroxide.

Many atmospheric chemistry models have a high bias in sulfur dioxide and a low bias in cloud cover compared with observations. Hains (2007) found that sulfur dioxide column content has a 55% high bias in the Environmental Protection Agency's (EPA) Community Multiscale Air Quality (CMAQ) model when run at a 12 km horizontal resolution and a 50% high bias in the Georgia Tech/Goddard Global Ozone Chemistry Aerosol Radiation and Transport (GOCART) model when run at a 2° latitude by 2.5° longitude resolution. Hains (2007) suggested that the high biases are due to an underestimation of sulfate conversion in clouds. Mueller et al. (2006) noted that CMAQ has a low cloud bias and high sulfur dioxide bias and used two alternative cloud parameterizations to improve the simulation. In their study the alternative parameterizations improved the frequency of clear sky and overcast sky conditions but still underestimated the frequency of partly cloudy sky conditions. Sulfur dioxide and sulfate biases decreased with the alternative parameterizations as additional clouds increased the rate at which sulfur dioxide was converted to sulfate. A high bias of total sulfur in the planetary boundary layer (PBL) remained and Mueller et al. (2006) stated that CMAQ might underestimate the removal of pollutants from the PBL by convective venting. Increasing convective venting causes pollutants to have longer lifetimes and be transported greater distances exacerbating air pollution downwind. Previous studies showed air quality models underestimating interstate transport of pollutants (e.g., Gilliland et al. (2008) and Godowitch et al. (2010) using CMAQ and Hogrefe et al. (2000) using the Urban Airshed Model, Variable-Grid Version (UAM-V)).

On the other hand, Lee et al. (2011) showed that GEOS-CHEM, a global chemistry model, reproduced the column content of SO_2 measured by aircraft or satellite instruments implying that the short lifetime was captured. Yu et al. (2007) has shown that CMAQ simulations at 12 km horizontal resolution have good agreement with SO_2 aircraft observations in Ohio River Valley power plant plumes at ~1000, but have a high bias below 700 m in the New York City and Boston urban plumes. Yu et al. (2007) suggested that this could be attributed to an overestimation of emissions from the New York City and Boston areas. It has also been shown that CMAQ simulations at 12 km horizontal resolution have a high SO_2 bias compared with ship observations off the coast of New England when the airflow is from the west and southwest (Yu et al., 2010). This high bias could be due to an overestimation of emissions in the Washington, DC, New York City, and Boston metropolitan areas (Yu et al., 2010) or a too slow removal rate in the model could produce the same bias.

Previous studies have shown that a sea breeze circulation can exacerbate air pollution levels. Evtyugina et al. (2006) showed that along the Portuguese west coast ozone levels are elevated when a sea breeze is present. Boucouvala and Bornstein (2003) found that peak ozone concentrations in southern California on high ozone days occur at the farthest inland location of a sea breeze's convergence zone. In Houston, high ozone episodes begin when the large-scale flow is offshore (Banta et al., 2005; Darby, 2005). As the bay breeze begins to develop stagnant conditions ensue allowing ozone and ozone precursors to accumulate before being advected further onshore as the bay breeze increases in intensity later in the afternoon (Banta et al., 2005; Darby, 2005).

With rapid increases in computing power in recent years, there have been a growing number of higher-resolution model simulations. The importance of increasing resolution in producing better-defined and more realistic mesoscale structures has been long recognized in the NWP community, since the horizontal resolution in operational models has been reduced from 300 to 400 km in middle 1950's to a few km today. In particular, many studies have shown benefits of using high-resolution NWP models to resolve frontal structures, orographical flows, and vertical circulations induced by surface inhomogeneities (see Mass et al., 2002 for review). Mass et al. (2002) explained that while it is difficult to prove that high-resolution simulations are more accurate due to the sparseness of observational sites, high-resolution simulations appear to produce more realistic weather structures.

High-resolution CMAQ modeling is also desirable for understanding the transport of air pollutants. Cohan et al. (2006) found that while air quality modeling at a horizontal resolution of 12 km is sufficient to determine regional-scale features of ozone changes to emissions reductions, finer resolution is necessary to capture localized variability. Jimenez et al. (2006) determined that a 2 km CMAQ simulation better simulates ozone concentrations in the presence of a sea breeze than 4 and 8 km simulations. Weijers et al. (2004) found evidence that the spatial scale of aerosol variability is below 1 km in urban areas. Sokhi et al. (2006) showed that CMAQ run at a horizontal resolution of 1 km reproduces temporal fluctuations in ozone well, but like coarse model simulations underpredicts daily maximum ozone and overpredicts nighttime ozone concentrations. Nevertheless, few numerical studies have been performed to examine the variability of air chemistry interacting with fair-weather cumulus clouds and sea-breeze circulations with horizontal resolutions below 1 km.

In the present study, we attempt to examine the above issues with state-of-the-art NWP and air quality models by pushing the horizontal resolution down to 0.5 km. The objectives of this study are to a) investigate how model resolution impacts the development of fair-weather cumulus clouds, the transport of pollutants through clouds, and sulfur dioxide to sulfate aerosol conversion in clouds in the model; and b) examine the effects of varying horizontal resolution on the development of the Chesapeake Bay breeze and the associated advection of air pollutants. These objectives are achieved by performing simulations with the Weather Research and Forecasting (WRF) model (Skamarock et al., 2008) coupled with the Urban Canopy model (UCM, Kusaka et al., 2001) and simulations with the CMAQ model (Byun and Schere, 2006) covering the Washington-Baltimore metropolitan areas from 1200 UTC 7 July to 1200 UTC 10 July 2007. This time period covers a period of fair-weather cumulus clouds (afternoon of 7 July), and one of the worst air pollution events of the decade (9 July) in which 8 h maximum ozone concentrations reached 114 ppbv downwind

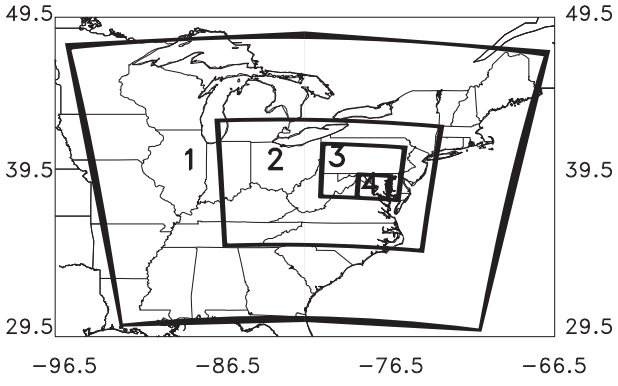

Fig. 1. Location of modeling domains 1, 2, 3, and 4, which have horizontal resolutions of 13.5, 4.5, 1.5, and 0.5 km, respectively.

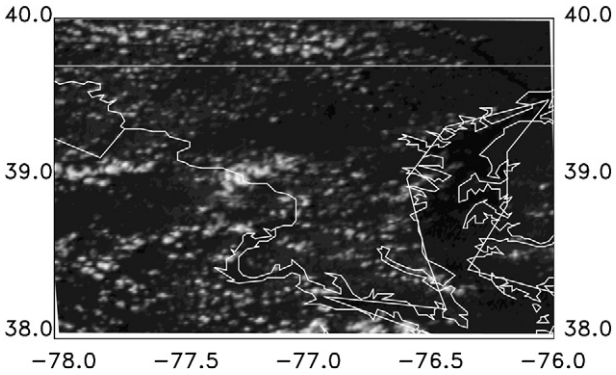

Fig. 2. GOES Visible satellite image at 2000 UTC 7 July 2007. White regions show locations of fair-weather cumulus clouds in the region. The white lines depict state borders and coastlines.

of Baltimore, MD near the Chesapeake Bay coastline in Edgewood, MD. Yegorova et al. (in press) analyzed this same air pollution event using the WRF model with online chemistry (WRF/chem) at 12 km resolution and observations. The air pollution event began with the passage of a cold front on 6 July 2007. Subsequently, an anticyclone developed and approached the Mid-Atlantic from the southeast and brought sunny, stagnant conditions to the region.

2. Model description

In this study, we use the Environmental Protection Agency's (EPA) Community Multiscale Air Quality (CMAQ) model, which is fed off-line by output from the Advanced Research WRF (WRF-ARW) model via the Meteorology-Chemistry Interface Processor (MCIP) (Otte and Pleim, 2010), to achieve the above-mentioned objectives.

2.1. Meteorological model and post processing

The WRF model is coupled with the Noah land surface model and the single layer Urban Canopy Model (UCM). The Noah scheme produces soil moisture, soil temperature, skin temperature, canopy water content, and the energy flux and water flux terms in the surface energy balance and surface water balance (Chen and Dudhia, 2001). The UCM improves the parameterization of physical processes involved in the exchange of heat, momentum, and water vapor in urban environments by including shadowing from buildings, reflection of short and longwave radiation, wind profile information in the canopy layer and a multi-layer heat transfer equation for roof, wall and road surfaces (Kusaka and Kimura, 2004). Other physics options that are used include a double-moment six-class microphysics scheme that calculates water vapor, cloud water, rain, cloud ice, snow, and graupel mixing ratio (Lim and Hong, 2010), the Mellor–Yamada–Janjic (MYJ) boundary layer parameterization (Janjic, 1994), and the Grell three-dimensional (3D) ensemble cumulus scheme, which expands on the Grell–Devenyi scheme (Grell and Devenyi, 2002) to allow subsidence in neighboring grid cells (Skamarock et al., 2008). The Grell 3D scheme is only used in the outermost domain.

Zhang et al. (2009) and Shou and Zhang (2010) used WRF-UCM simulations to show that upstream landuse can exacerbate the urban heat island (UHI) effect. We use the WRF-UCM with the same domain along with CMAQ to investigate the impact of model resolution on sulfur dioxide oxidation in fair-weather cumulus clouds, the Chesapeake Bay breeze, the dispersion of pollutants, and ozone formation. The model is run at 13.5, 4.5, 1.5, and 0.5 km horizontal resolution from 1200 UTC 7 July to 1200 UTC 10 July 2007 with dimensions of 181 × 151, 244 × 196, 280 × 247, and 349 × 349 grid cells, respectively (see Fig. 1 for the model domains). All of the domains use 30 layers in the vertical with 20 layers in the lowest 2 km. The NCEP Final Reanalysis is used for the model initial

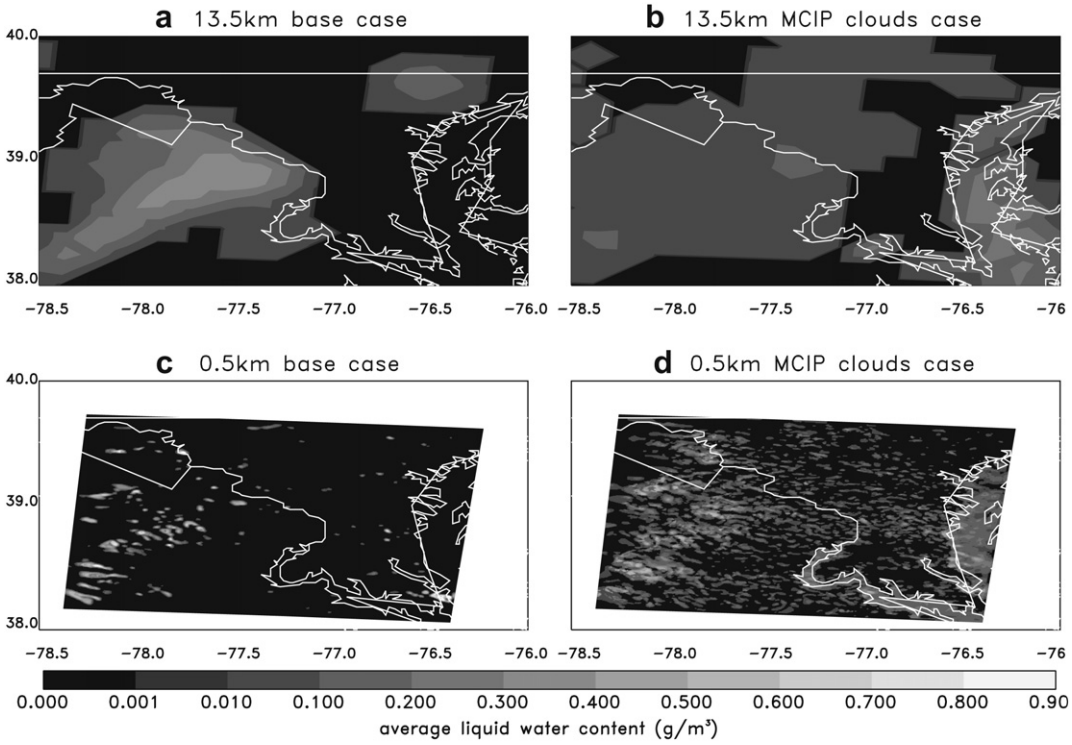

Fig. 3. Cloud average liquid water content (g/m^3) used in CMAQ's aqueous chemistry scheme for the a) 13.5 km base case, b) 13.5 km MCIP clouds case, c) 0.5 km base case, and d) 0.5 km MCIP clouds case at 2000 UTC 7 July 2007. The white lines depict state borders and coastlines. The high resolution MCIP clouds most nearly resemble observations (Fig. 2).

and outermost lateral boundary conditions. In the present study, Version 3.1.1 of the WRF model is used instead of Version 2.2.1, used by Zhang et al. (2009) and Shou and Zhang (2010). In addition, in order to examine the impact of varying model resolutions on the simulated air chemistry, one-way feedback is used instead of two-way feedback between the domains. Two-way feedback involves information being exchanged bi-directionally between the finer and coarser grids, whereas one-way feedback only involves information exchange from the coarse grid to the finer grid (Zhang et al., 1986).

A mass conservation problem was identified in the 0.5 km resolution domain of the WRF-UCM and CMAQ simulations. A mass balance analysis from a CMAQ simulation with chemistry turned off revealed a change in mass of chemical species that was inconsistent with model calculated sources, sinks, and fluxes. After analysis of the WRF-UCM output, we determined that the mass non-conservation was caused by waves reflecting off the top of the model domain. Fortunately, WRF-UCM includes damping options to minimize unrealistic reflections at the top of the model. WRF-UCM was re-run with gravity wave damping (Klemp et al., 2008) and vertical velocity damping (Skamarock et al., 2008) with respective damping coefficients of 0.2 and 0.3. These changes minimize unrealistic reflections at the top of the modeling domain and loss in mass.

Version 3.4 of MCIP was used to ingest the WRF-UCM outputs and create input files for processing emissions data and running air chemistry simulations. This step requires modifying MCIP to write out the percentage of each WRF-UCM grid cell that is urban. Urban fraction is used in CMAQ to calculate vertical diffusion. This model update is available beginning in Version 3.5_beta of MCIP.

2.2. Emissions

Emissions input files are created with the Sparse Matrix Operator Kernel Emissions (SMOKE) modeling system (Houyoux and Vukovich, 1999). Because a 2007 emissions inventory is not yet available, projected annual 2009 emissions from U.S. Regional Planning Organizations (RPOs) are processed with SMOKE to create hourly emissions input files for CMAQ. The annual 2009 projected emissions from the U.S. RPOs were grown from annual 2002 emissions and include estimated emissions changes due to growth and emissions controls that were expected to be implemented by 2009.

Area source emissions input to SMOKE are annual, countywide emissions, and are temporally and horizontally spatially distributed with SMOKE to create hourly gridded CMAQ emissions input files. Annual emissions are distributed based on the time of day, day of the week, and season based on temporal emissions distributions provided by the U.S. RPOs. Countywide area emissions are horizontally distributed based on gridded highly detailed landuse patterns from a spatial surrogate file. These landuse patterns are obtained from shapefiles that describe landuse from the 2000 census, National Land Cover Characteristics Data, and other spatial sources available from EPA's Emissions Modeling Clearinghouse. The shapefiles are input into the Multimedia Integrated Modeling System (MIMS) Spatial Allocator (Eyth and Brunk, 2005) to create a spatial surrogate file.

Point source emissions data are annual emissions for a specific location, and are temporally and spatially distributed in the vertical with SMOKE. Similar to the area emissions, the point source emissions are distributed based on temporal emissions distributions provided by the U.S. RPOs, except for power point sources, which are temporally distributed based on continuous emissions monitoring (CEM) observations. Also, point sources are vertically distributed based on temperature and velocity of the emissions, stack height, and meteorological conditions.

Mobile and biogenic emissions are also processed to create CMAQ emissions input files. Mobile emissions are created with MOBILE6 (U.S. Environmental Protection Agency, 2003) and biogenic emissions are processed with the Biogenic Emissions Inventory System (BEIS) Version 3.12 based on meteorology and landuse (Vukovich and Pierce, 2002). MOBILE6 and BEIS are coupled with SMOKE.

2.3. Air quality model description

The EPA's CMAQ model Version 4.6 (Byun and Schere, 2006) is used to investigate the role of fair-weather cumulus clouds in the

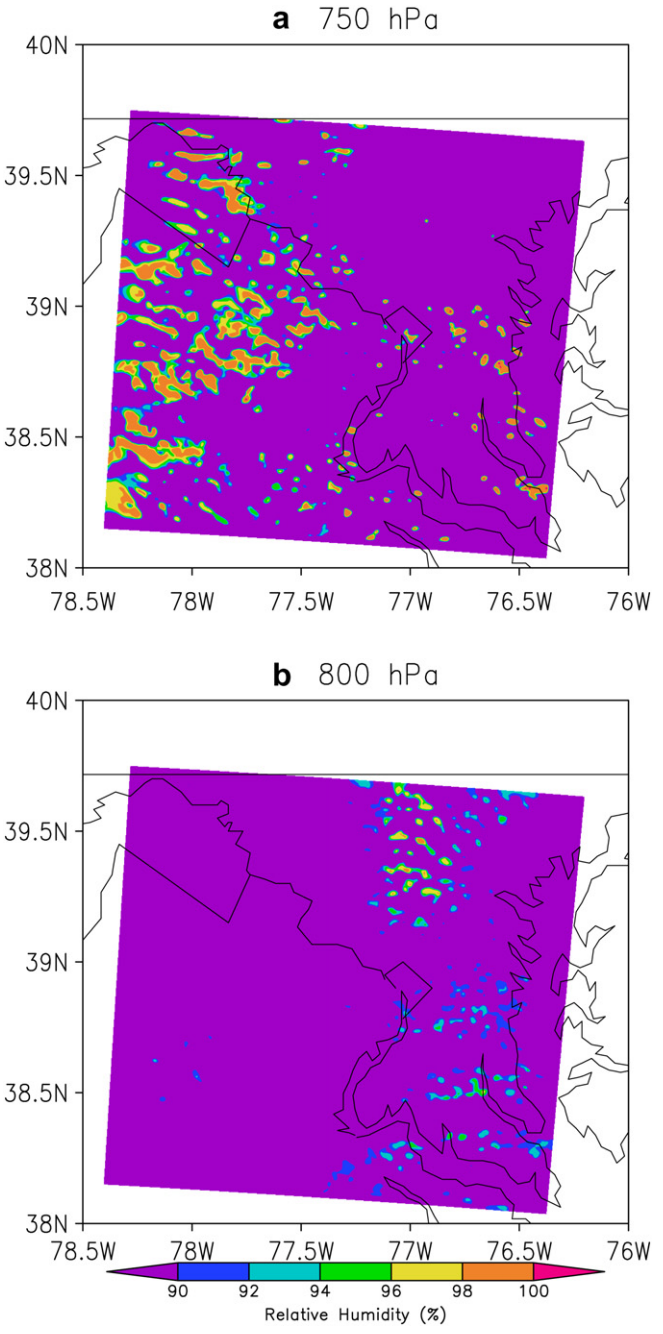

Fig. 4. Relative humidity (%) for the 0.5 km horizontal resolution simulation at 2000 UTC 7 July 2007 at a) 750 hPa and b) 800 hPa.

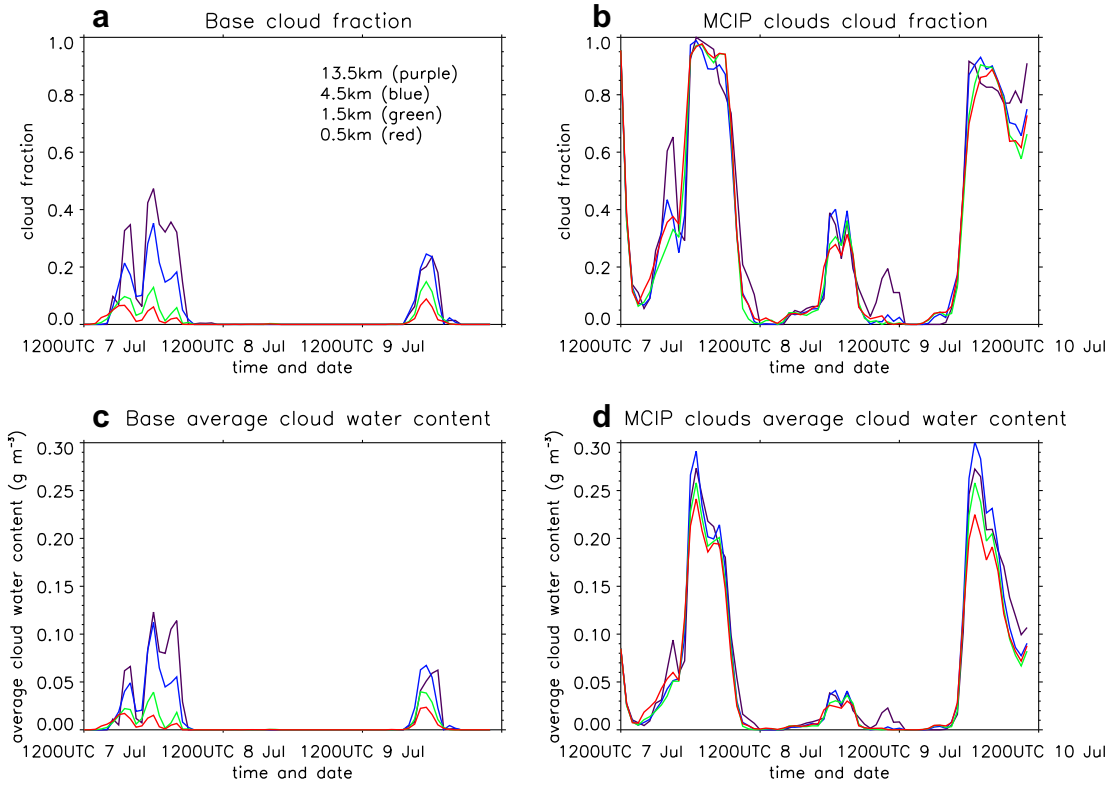

Fig. 5. Time-series of model cloud fraction for the a) base case and b) MCIP clouds case and average cloud liquid water content (g/m^3) for the c) base case and d) MCIP clouds case for the 13.5, 4.5, 1.5, and 0.5 km horizontal resolution simulations averaged over the 0.5 km domain from 1200 UTC 7 July to 1200 UTC 10 July 2007.

conversion of sulfur dioxide to sulfate aerosols and how the bay breeze influences the dispersion of pollutants and the formation of ozone. Here the model is run with the following user options: (1) a density based mass-conserving Piecewise Parabolic Method advection scheme (Colella and Woodward, 1984); (2) the Carbon Bond-05 gas-phase chemical mechanism (Yarwood et al., 2005); (3) the Asymmetric Convective Model Version 2 (Pleim, 2007) for vertical diffusion; and (4) a cloud module that uses the Regional Acid Deposition Model (Chang et al., 1987) to calculate the aqueous phase chemistry and the Asymmetric Convective Model (Pleim and Chang, 1992) to compute convective mixing. CMAQ is run with the same vertical resolution as the WRF-UCM simulations. Chemical initial and boundary conditions come from a Model for Ozone and Related chemical Tracers, Version 4 (MOZART-4) simulation (Emmons et al., 2010). Also, the 13.5 km resolution domain simulation begins 2 weeks prior to 1200 UTC 7 July 2007 to spin up the chemistry of the atmosphere for the species unavailable from global model output files used for chemical initial conditions.

Several model improvements are made to CMAQ based on Castellanos (2009), Castellanos et al. (in press), and Odman and Hu (2009). The non-urban minimum eddy diffusion coefficient used in CMAQ is reduced from 0.5 to 0.1 $m^2\ s^{-1}$ to be consistent with micrometeorological observations and to improve model results (Castellanos, 2009; Castellanos et al., in press). Also, the CO dry deposition velocity is reduced from 0.001 to 0.0 $m^2\ s^{-1}$, turning off CO dry deposition, which agrees better with observations (Castellanos, 2009). Bug fixes to the advection and horizontal diffusion schemes are implemented following Odman and Hu (2009). Finally, the CMAQ code is modified to output the flux of each species due to horizontal advection to adjacent grid cells.

CMAQ uses cloud properties to calculate photolysis rates and aqueous chemistry reactions. However, the representation of these cloud properties differs between the photolysis and aqueous chemistry schemes (Byun and Schere, 2006; Otte and Pleim, 2010). The cloud properties used in CMAQ's aqueous chemistry scheme consist of three-dimensional cloud water, rain, cloud ice, snow, and graupel mixing ratio from explicit clouds calculated in the WRF-UCM (Byun and Schere, 2006). When the horizontal resolution is coarser than 8 km, CMAQ adds parameterized clouds calculated in CMAQ's cloud module to the explicit clouds (Byun and Schere,

Table 1
10th percentile, median, and 90th percentile 24 h average sulfur dioxide (ppbv) and sulfate ($\mu g/m^3$) concentrations at Beltsville, MD from 1200 UTC 7 July to 1200 UTC 8 July. Values reflect variability in space for a 1640.25 km^2 region surrounding the measurement site and are shown as a function of resolution and for the base and MCIP clouds simulations. The observed 24 h average SO_2 concentration at Beltsville, MD was 2.01 ppbv.

	Base SO_2 (ppbv)	MCIP clouds SO_2 (ppbv)	Base SO_4 ($\mu g/m^3$)	MCIP clouds SO_4 ($\mu g/m^3$)
13.5 km	3.32, 3.85, 7.96	3.16, 3.69, 7.77	4.73, 5.62, 6.22	5.70, 6.17, 7.16
4.5 km	2.66, 3.40, 4.27	2.62, 3.35 4.19	4.05, 5.29, 5.99	4.60, 4.60, 6.20
1.5 km	2.60, 4.16, 5.30	2.55, 4.06, 5.21	4.12, 5.36, 5.86	4.57, 5.95, 6.39
0.5 km	3.17, 3.97, 4.63	2.95, 3.72, 4.36	4.59, 5.49, 5.94	5.59, 6.58, 7.12

Table 2
10th percentile, median, and 90th percentile 24 h average sulfur dioxide (ppbv) and sulfate ($\mu g/m^3$) concentrations at Essex, MD from 1200 UTC 7 July to 1200 UTC 8 July. Values reflect variability in space for a 1640.25 km^2 region surrounding the measurement site and are shown as a function of resolution and for the base and MCIP clouds simulations. The observed 24 h average SO_2 concentration at Essex, MD was 2.45 ppbv.

	Base SO_2 (ppbv)	MCIP clouds SO_2 (ppbv)	Base SO_4 ($\mu g/m^3$)	MCIP clouds SO_4 ($\mu g/m^3$)
13.5 km	4.02, 4.91, 6.48	3.85, 4.80, 6.33	4.94, 5.85, 6.14	5.84, 6.42, 6.94
4.5 km	4.00, 7.32, 10.64	3.88, 7.18, 10.52	5.06, 6.56, 7.75	5.75, 7.23, 8.33
1.5 km	3.53, 5.53, 12.94	3.38, 5.36, 12.83	5.06, 6.56, 7.75	5.72, 6.45, 8.34
0.5 km	3.63, 4.99, 13.58	3.40, 4.78, 13.44	4.99, 5.69, 7.51	6.11, 6.75, 8.36

2006). The cloud properties used in CMAQ's photolysis scheme are two dimensional and consist of cloud top, cloud base, cloud fraction, and the total cloud water content averaged between the cloud top and cloud base (Otte and Pleim, 2010). These variables are diagnosed in MCIP using an algorithm based on a relative humidity (RH) threshold as described by Byun et al. (1999).

Differences in the representation of cloud properties between the photolysis and aqueous chemistry schemes are analyzed and simulations using the photolysis clouds in the aqueous chemistry scheme, hereafter referred to as MCIP clouds simulations, are performed to determine the sensitivity of sulfur dioxide and sulfate concentrations to the representation of cloud properties in the WRF-MCIP-CMAQ system. In order to perform the MCIP clouds simulations, MCIP is modified so that the input fields of the aqueous chemistry scheme use the same cloud properties as the photolysis cloud properties. Three-dimensional cloud fraction and total cloud water content are calculated in the same way as the photolysis scheme's two-dimensional cloud fraction and total water content but are not averaged in the vertical between the cloud base and cloud top. Total cloud water is then multiplied by the cloud fraction to obtain a new total cloud water content for use in CMAQ's aqueous chemistry scheme in the MCIP clouds simulations. The MCIP clouds simulations use the same graupel, ice, snow, and rain content as the base case, i.e., from the WRF model output. The graupel, ice, snow, and rain content are then subtracted from the new total cloud water content variable to obtain cloud liquid water content that is used in CMAQ. The 13.5 km MCIP clouds simulation is run with CMAQ calculated parameterized clouds turned off in the aqueous chemistry scheme as they are not needed since the MCIP RH-based clouds are calculated at all resolutions and includes parameterized clouds.

3. Results

In this section, we evaluate how model simulations with different horizontal resolutions affect the development of fair-weather cumulus clouds, the transport of pollutants through clouds, and sulfur dioxide to sulfate aerosol conversion in clouds; and then investigate the impact of varying horizontal resolution on the development of the Chesapeake Bay breezes and the associated advection of air pollutants.

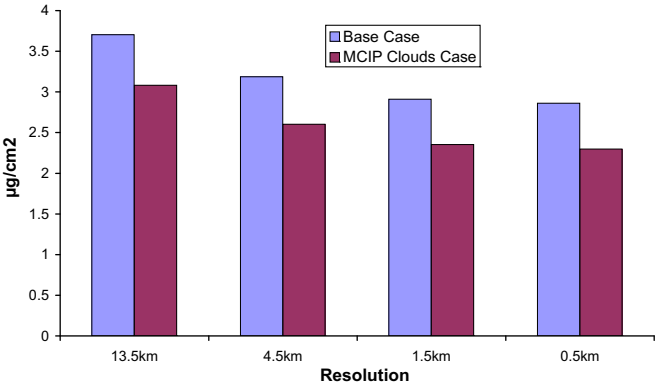

Fig. 7. Surface to 215 hPa SO_2 column (µg/cm^2) at 1200 UTC 8 July 2007 averaged over the innermost domain for the base and MCIP clouds case simulations at 13.5, 4.5, 1.5, and 0.5 km horizontal resolutions. The smaller column content should bring CMAQ into better agreement with observations (Hains 2009; Lee et al., 2011).

3.1. Impact of fair-weather cumulus clouds

Fair-weather cumulus clouds, which play a role in converting sulfur dioxide to sulfate aerosols, developed during the afternoon of 7 July 2007. A Geostationary Operational Environmental Satellite (GOES) visible image at 2000 UTC is shown in Fig. 2 and the average total cloud water content used in CMAQ's aqueous phase chemistry scheme from the 13.5 and 0.5 km resolution base and MCIP clouds simulations are compared in Fig. 3. The cloud properties from the MCIP clouds simulations better agree with satellite observations, while the base case simulations underestimate the spatial coverage

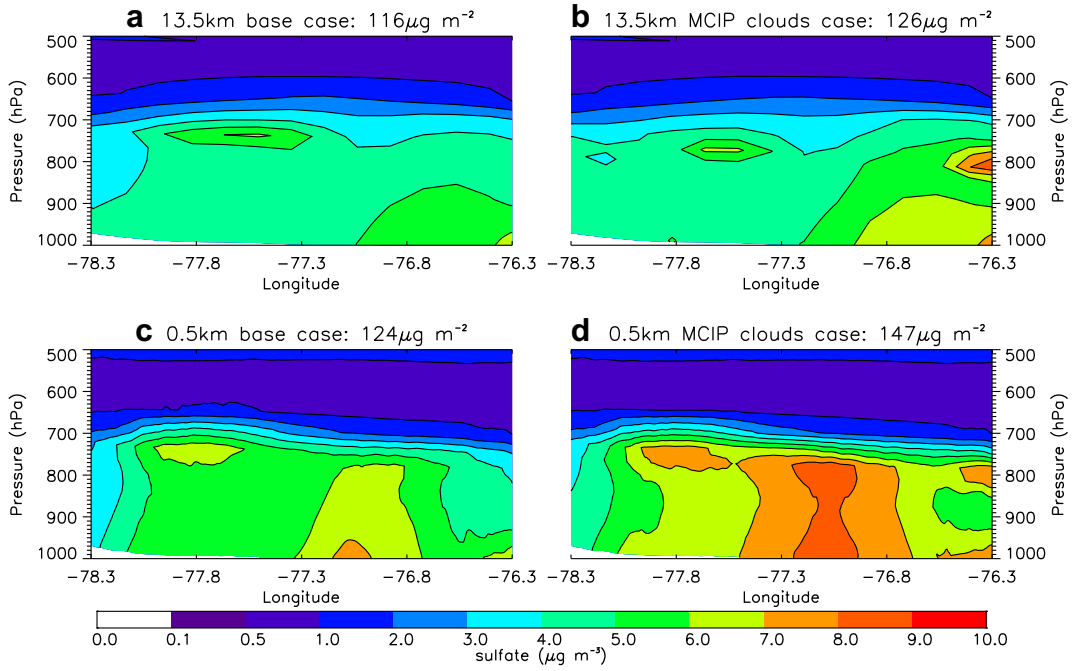

Fig. 6. West–east cross section of sulfate aerosols (µg/m^3) averaged over the north–south direction covering the area of the 0.5 km domain for the a) 13.5 km base case, b) 13.5 km MCIP clouds case, c) 0.5 km base case, and d) 0.5 km MCIP clouds case at 2000 UTC 7 July 2007. Fair-weather cumulus clouds are present at this time. The surface to 500 hPa sulfate column averaged over the innermost domain is shown above each figure.

of clouds. The 13.5 km resolution simulation is unable to resolve small, fair-weather cumulus clouds, as expected, and tends to produce smooth cloud fields, e.g., as shown by a single cloud system in Fig. 3a. RH maps from the 0.5 km resolution WRF simulation show many moist bubbles at 750 and 800 hPa (Fig. 4), two levels where fair-weather cumulus clouds are found. In these regions of high RH, water vapor is close to condensing to form clouds. The large spatial differences between Figs. 3c, 3d, 4a, and 4b show the sensitivity of model calculated fair-weather cumulus clouds to small variations in RH. These differences illustrate the difficulties involved in accurately diagnosing cloud properties in numerical models. The short spin-up time (8 h) may also contribute to the biases in model cloud cover. It can be seen from Fig. 5 that the MCIP clouds simulations have larger cloud fractions and average total cloud water content at all resolutions than in the base case. As the model resolution increases in the base case, the cloud fraction over the innermost domain on 7 July and 9 July decreases, and the clouds that do form have lower total water content (Fig. 5).

The simulated sulfur dioxide is compared to surface measurements from the EPA's Air Quality System (AQS) at two locations. The observed 24 h average sulfur dioxide concentrations from 1200 UTC 7 July to 1200 UTC 8 July at Beltsville, MD (39.06°N, 76.88°W) and Essex, MD (39.31°N, 76.47°W) are 2.01 and 2.45 ppbv, respectively. The model ground-level sulfur dioxide and sulfate aerosol concentrations for the base and MCIP clouds cases are shown in Table 1 for Beltsville and Table 2 for Essex. The CMAQ simulations have a high bias in sulfur dioxide at the measurement sites at all resolutions at both sites and for both the base and MCIP clouds cases. The higher resolution simulations have larger median SO_2 concentrations than the 13.5 km simulations around Essex because the higher resolution runs simulate stagnation downwind of emissions sources southeast of Essex causing pollution to accumulate. Observed median and 10th and 90th percentile sulfur dioxide concentrations for the month of July 2007 were 1.1, 0.2, and 4.2 ppbv, respectively at Beltsville and 3, 1, and 9 ppbv, respectively at Essex. It can be seen from Tables 1 and 2 that mean sulfur dioxide concentrations in the MCIP clouds simulations are slightly lower (1–6%) and sulfate concentrations are higher (7–20%) than the base case simulated sulfur dioxide and sulfate. More clouds in the MCIP clouds case cause more sulfur dioxide to be converted to sulfate aerosols. Since the PBL is well mixed, many sulfate aerosols formed in clouds aloft are transported downward to the surface.

Fig. 6 displays west-east cross sections of sulfate aerosols averaged over the north-south direction covering the innermost domain at 2000 UTC 7 July when fair-weather cumulus clouds are present in the 13.5 and 0.5 km resolution base and MCIP clouds simulations. It can be seen that more sulfate aerosols are present in the 0.5 km simulation. Even though the cloud fraction is lower and the liquid water content of clouds that do form is lower in the 0.5 km base case simulation than in the 13.5 km base case

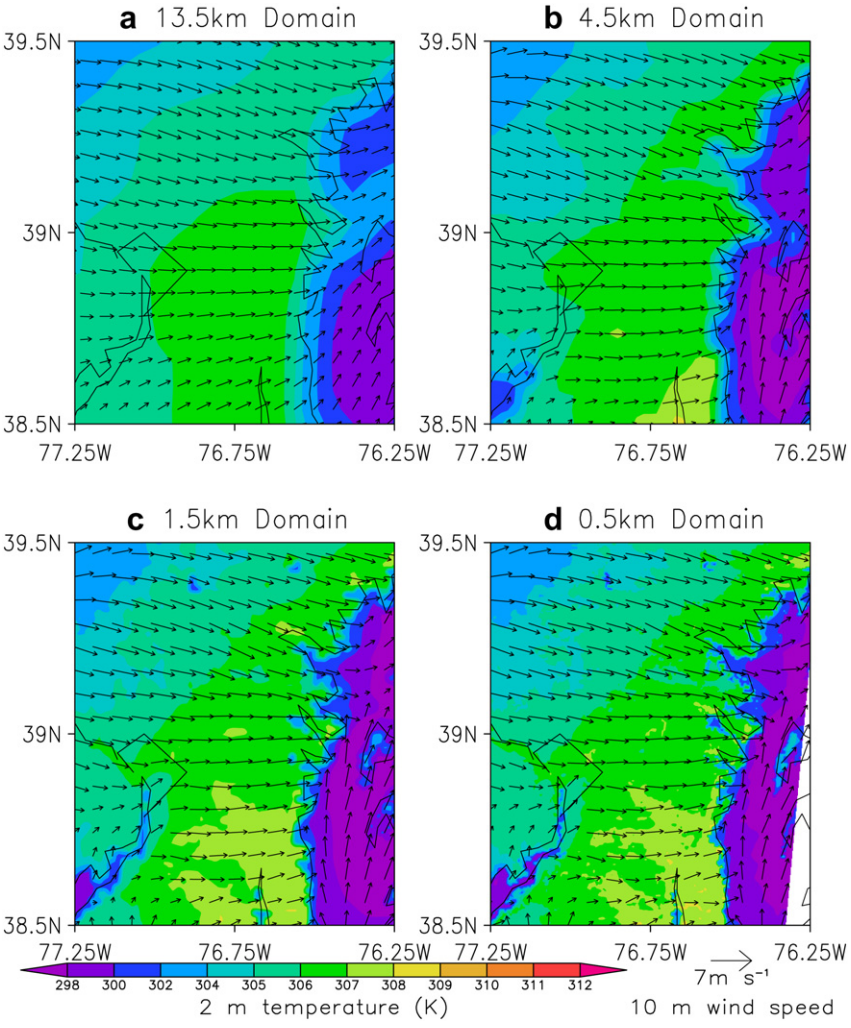

Fig. 8. 2 m temperature (K) and 10-m wind speeds for the a) 13.5, b) 4.5, c) 1.5, and d) 0.5 km horizontal resolution simulations at 1400 UTC (0900 EST) 9 July 2007.

simulation, more sulfur dioxide is being converted to sulfate aerosols in the 0.5 km resolution simulation. Apparently, higher resolution simulations cause more sulfur dioxide to be transported vertically into the clouds where it is converted to sulfate aerosols, and as expected, updrafts occur preferentially under clouds. Updraft speeds also increase as the resolution increases. At 2000 UTC 7 July the 4.5, 1.5, and 0.5 km resolution base case simulations averaged over the innermost domain have mass fluxes at 910 hPa that are 1.8, 7.5, and 20.3 times larger than the 13.5 km base case mass flux; these updraft calculations include vertical advection but not vertical diffusion. As expected, the SO_2 to sulfate conversion rates are also sensitive to cloud amount. Sulfate aerosols change noticeably between the MCIP clouds and base cases. More sulfate aerosols are present in the MCIP clouds case simulations due to the presence of more clouds(Fig. 6).

Sixteen hours later (i.e., at 1200 UTC 8 July), there is noticeably less sulfur dioxide present at higher resolutions (Fig. 7). Specifically, the surface to 215 hPa sulfur dioxide columns at 1200 UTC 8 July, averaged over the innermost domain for the 4.5, 1.5 and 0.5 km resolution base case simulations are 14, 21, and 23% smaller than that from the 13.5 km resolution base case simulation (Fig. 7). However, differences in the amount of sulfate aerosols between the base and MCIP clouds simulations are small. The base case sulfate column of the 4.5 km simulation is 3% larger than in the 13.5 km simulation, while the 1.5 and 0.5 km simulations' sulfate columns are 4% smaller.

Net flux of total sulfur (sulfur dioxide, sulfate aerosols, and sulfuric acid) integrated over the vertical extent of the model into and out of the area of the innermost domain for each simulation will now be analyzed to examine why the column content sulfur dioxide decreases as the horizontal resolution increases. While all of the CMAQ simulations have a net flux of total sulfur out of the area during the first 24 h of simulations, due partly to sulfur from emissions in the innermost domain being transported out of the domain, the magnitude of the net outward flux increases as the resolution increases. When integrating over the depth of the model the 4.5, 1.5, and 0.5 km resolution simulations have 52, 68, and 70% more sulfur leaving the area than the 13.5 km resolution.

There is a net import of sulfur in the PBL and a net export in the free troposphere. As the model resolution increases, more sulfur is transported aloft and vented out of the PBL to the free troposphere where winds are stronger causing the pollutants to be transported downwind more quickly. Fig. 7 shows that as the resolution increases, sulfur dioxide integrated from the surface to 215 hPa within the innermost domain decreases due to more sulfur dioxide being converted to sulfate aerosols and more being transported out of the area of the innermost domain. Also, the MCIP clouds simulations have less column integrated sulfur dioxide than the base

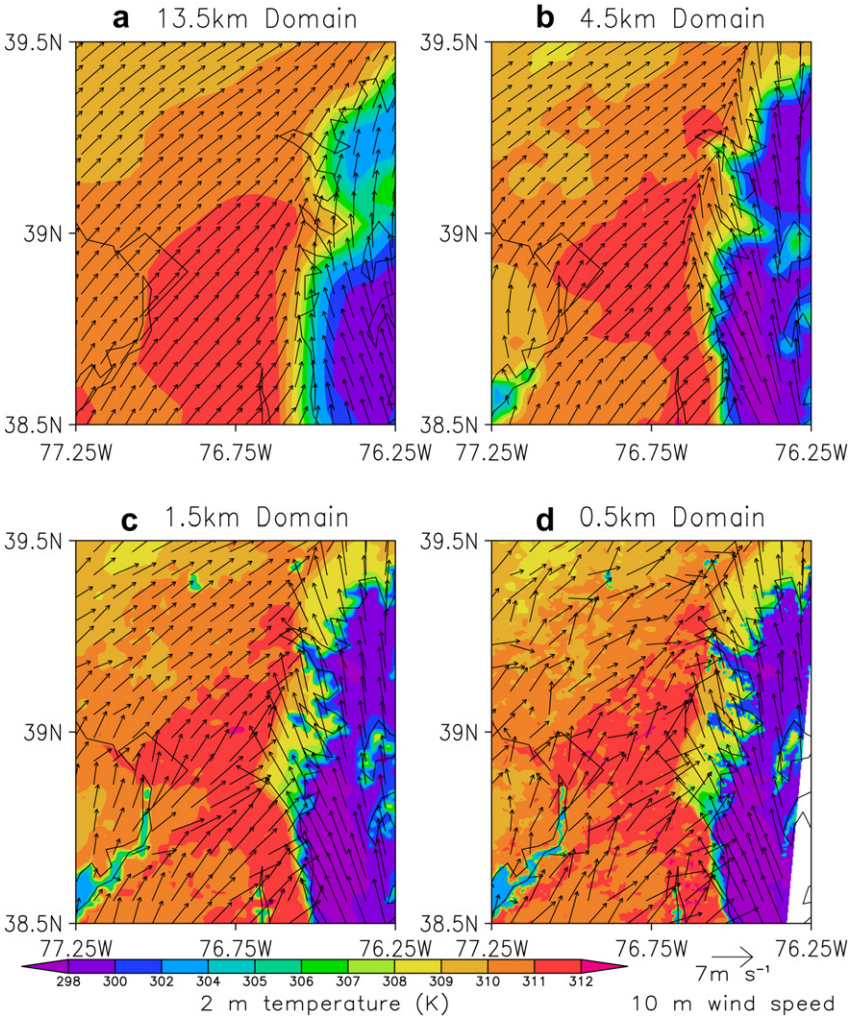

Fig. 9. 2 m temperature (K) and 10 m wind speeds for the a) 13.5, b) 4.5, c) 1.5, and d) 0.5 km horizontal resolution simulations at 1900 UTC (1400 EST) 9 July 2007.

case simulations due to the presence of more clouds, which causes more sulfur dioxide to be oxidized to form sulfate aerosols.

3.2. Impact of the Chesapeake Bay breezes

Coarser resolution model simulations are unable to capture large abrupt changes in surface characteristics, such as land-water boundaries of fronts. In the early morning of 9 July 2007, the synoptic-scale winds were westerly. By mid-morning (i.e., at 1400 UTC or 0900 EST), stagnation is present in the northern Chesapeake Bay (downwind of Baltimore, MD) in the 4.5, 1.5, and 0.5 km resolution simulations (Fig. 8) as a result of the wind direction changing from a westerly to southeasterly direction as the bay breeze sets up (Fig. 9). This stagnation allows ozone and ozone precursors to accumulate east of Baltimore and Washington, DC over the bay. The 13.5 km resolution simulation, however, does not generate stagnation over the bay and produces a weaker bay breeze that starts later due to a smaller temperature gradient along the coastline. Instead, the winds over the northern Chesapeake Bay in the 13.5 km resolution simulation shift from a westerly to

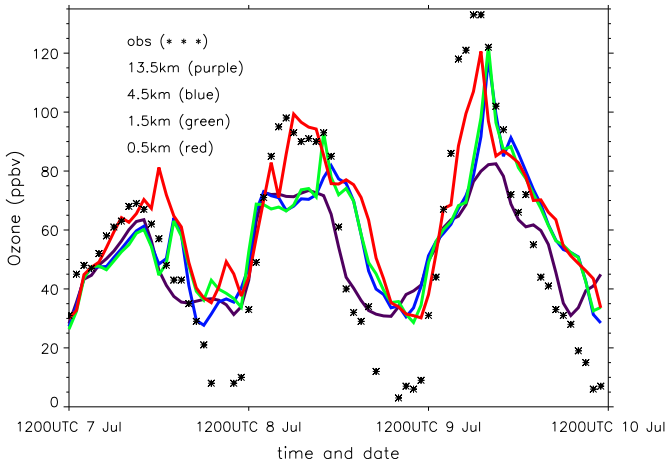

Fig. 11. Ozone (ppbv) time-series at Edgewood, MD from AQS measurements and the 13.5, 4.5, 1.5, and 0.5 km resolution simulations at the lowest model level from 1200 UTC 7 July to 1200 UTC 10 July 2007.

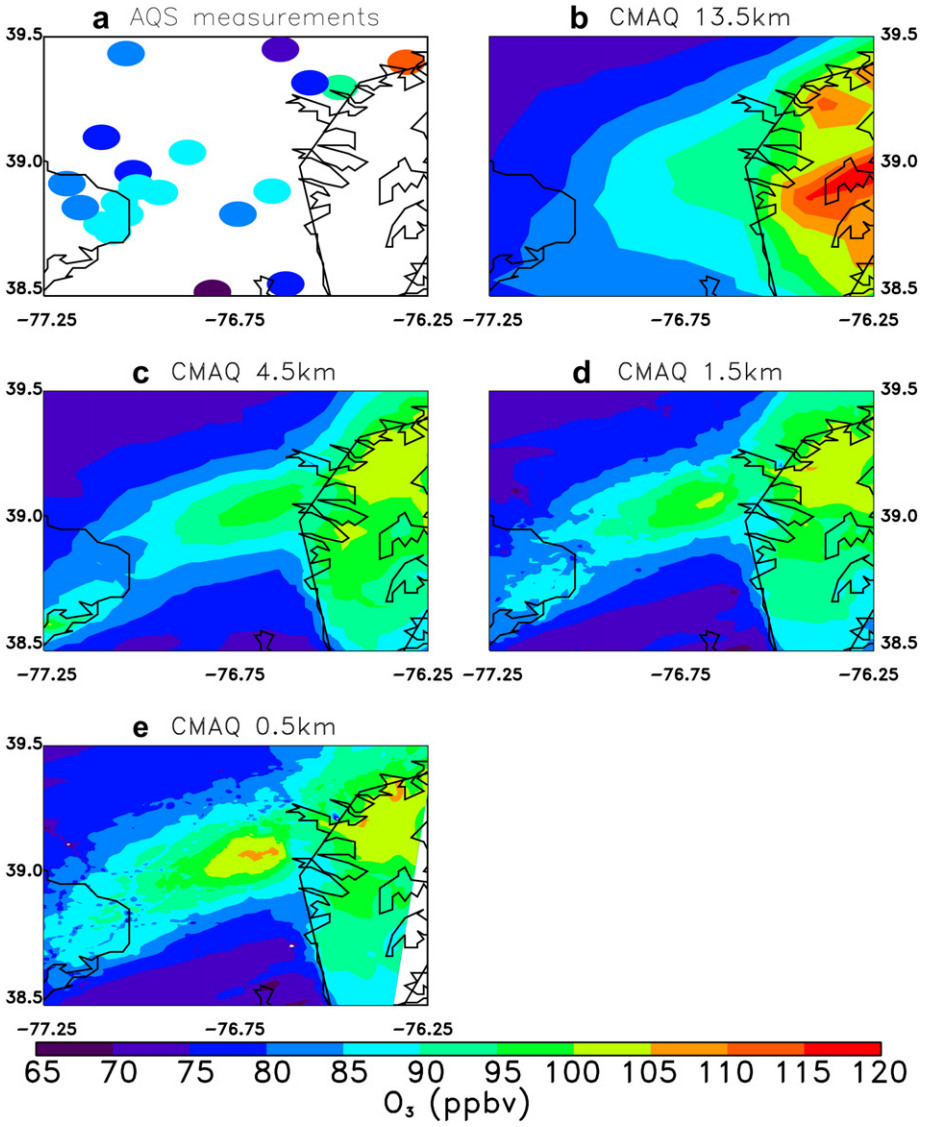

Fig. 10. 8 h maximum ozone concentrations (ppbv) from a) EPA's Air Quality System (AQS) observations and the b) 13.5, c) 4.5, d) 1.5, and e) 0.5 km horizontal resolution simulations at the lowest model level on 9 July 2007. The white lines depict state borders and coastlines.

southwesterly direction by mid-morning. By mid-afternoon, the winds at all resolutions shift to a southerly direction. At 1900 UTC, it can be seen that as the resolution increases, the bay breeze increases in strength, and its convergence zone pushes farther inland (Fig. 9). The area of land grid boxes with easterly winds at 1900 UTC near the surface between 76.5–76.25°W and 38.5–39.5°N for the 13.5, 4.5, 1.5, and 0.5 km resolution domains are 182, 851, 1040, and 1087 km^2, respectively.

Air quality was poor on 9 July 2007, and mean ozone concentrations from all of the CMAQ simulations agree well with EPA's AQS observations at 30 sites in the innermost domain (see Fig. 10). The 8 h maximum ozone concentrations for the 13.5 and 4.5 km resolution simulations have mean low biases of 1.9 and 1.3 ppbv, respectively, whereas the 1.5 and 0.5 km simulations have mean high biases of 0.56 and 1.0 ppbv, respectively. A notable improvement in the centered root mean squared error is obtained as the resolution increases from 13.5 to 4.5 km. The centered root mean squared error of the 8 h maximum ozone is 9.60, 6.92, 6.77, and 6.92 ppbv for the 13.5, 4.5, 1.5, and 0.5 km simulations, respectively.

The highest 8 h maximum ozone measured on 9 July in the innermost domain occurred at Edgewood, MD (39.4°N, 76.3°W), the northeastern-most measurement point depicted in Fig. 10a located on the northern coast of the Chesapeake Bay. Its value was 114 ppbv while the model simulates 8 h maximum concentrations of 75, 91, 92, and 96 ppbv at 13.5, 4.5, 1.5, and 0.5 km resolution, respectively. The low bias may be partially due to a low bias in emissions. Projected 2009 emissions are used, which may contain emissions controls, or emissions reductions, which had not been implemented by July 2007. A time series of ozone observations and model results at Edgewood shows that the model has a low bias during the day on 9 July at all resolutions with the 13.5 km resolution simulation performing the worst (Fig. 11). The high bias at night may be attributed to the dry deposition velocity of pollutants being too slow in CMAQ. Y. Choi (personal communication) found that adjusting the aerodynamic resistance with improved forest canopy heights increases dry deposition velocity and brings CMAQ into better agreement with observations in the Northeastern US. While the increased ozone dry deposition velocities improved CMAQ simulated ozone in the Southeastern US, a high bias still remained (Y. Choi, personal communication). The high bias in the southeast corresponded with a high bias in formaldehyde and more NO_x sensitive regions than observations reveal, which may be due to a high bias in biogenic emissions (Y. Choi, personal communication). The 4.5, 1.5, and 0.5 km resolution simulations come into

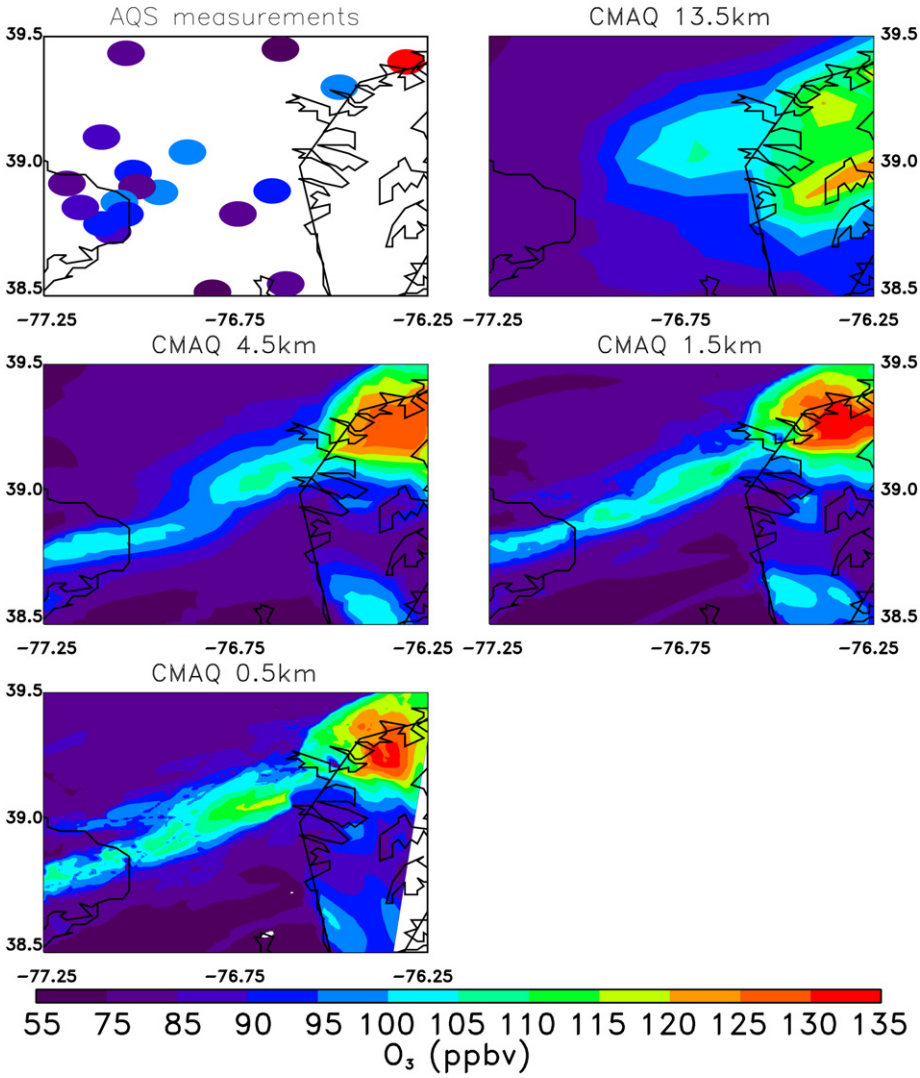

Fig. 12. Ozone concentrations (ppbv) from a) AQS observations and the b) 13.5, c) 4.5, d) 1.5, and e) 0.5 km horizontal resolution simulations at the lowest model level at 1900 UTC 9 July 2007. The white lines depict state borders and coastlines.

better agreement with the observations at Edgewood on 9 July because they simulate mid-morning stagnation over the northern Chesapeake Bay causing pollutants to accumulate, a late-morning bay breeze causing pollutants to converge over Edgewood, and afternoon advection by southerly winds causing additional ozone that had built up over the bay to be transported to Edgewood (Fig. 12). The 13.5 km resolution simulation does not produce a bay breeze convergence zone over Edgewood.

The 13.5 km CMAQ simulation has higher 8 h maximum ozone concentrations near the surface over the Chesapeake Bay than over land (Fig. 10) even though less stagnation is present over the bay during the morning in the 13.5 km resolution simulation (Fig. 8). The early morning stagnation seen in the higher resolution runs causes localized high concentrations over the bay. However, concentrations decrease later in the day as the bay breeze transports the pollutants northward and as it limits the west to east transport across the coastline. Since the simulated bay breeze is weaker at 13.5 km, more pollutants flow near the surface over the bay where the PBL is shallow over the cool water surface. In addition, it appears that more pollutants are directly emitted over the bay in coarser resolution simulations due to the failure to properly resolve the coastline. Emissions in a grid cell that straddle the coastline can appear to be emitted over the water, but in reality they are emitted over land. Fig. 13 depicts a west–east cross section of CO for the 13.5, 4.5, 1.5, and 0.5 km resolution base case simulations at 1900 UTC 9 July, in which the coastline is located at 76.42°W. The cross section is located at 39.1°N, which includes the area of high ground-level ozone concentrations between Washington, DC and Baltimore, MD in the 0.5 km resolution simulation. One can see that the 0.5 km resolution model run simulates a stronger bay breeze that inhibits pollutants from being transported eastward over the water near the surface. Instead, pollutants are lofted and then transported eastward. The high resolution simulation shows a local maximum in CO mixing ration near the top of the PBL, as has been observed for CO and O_3 in this area (Castellanos et al., in press; Taubman et al., 2006). Pollutants lofted out of the PBL have a longer lifetime and greater range of influence. The lofting associated with the bay breeze causes lower pollutant concentrations near the surface over the water in the higher resolution simulations (Fig. 10). The simulated maximum 8 h surface ozone concentrations over the Chesapeake Bay on 9 July are 116, 105, 105, and 106 ppbv for the 13.5, 4.5, 1.5, and 0.5 km resolution simulations, respectively. Even though the bay breeze increases in strength with increasing resolution, the bay breezes in the 4.5 and 1.5 km resolution simulations are strong enough to prevent pollutants emitted over land in the afternoon from being transported over the water near the surface similar to the 0.5 km resolution simulation. This results in similar maximum 8 h ozone concentrations over the water. The mean 8 h maximum ozone concentrations over land between 77.25–76.25°N and 38.5–39.5°N are 83.7, 82.4, 82.4, and 84.1 ppbv, and the mean 8 h maximum ozone concentrations over water with the same boundaries are 105.0, 96.4, 94.0, and 94.2 ppbv for the 13.5, 4.5, 1.5, and 0.5 km resolution domains, respectively. As the resolution increases, 8 h maximum ozone concentrations increases near the bay breeze convergence zone and decrease over the entire Chesapeake Bay.

4. Discussion

In previous studies, CMAQ has shown a weakness in modeling partly cloudy sky conditions (Mueller et al., 2006) and the sulfur budget (Hains, 2007; Mueller et al., 2006). This work shows we can improve on these problems by using diagnosed clouds that agree with observations and by increasing the model resolution. CMAQ's aqueous chemistry scheme and photolysis scheme generate dramatically different cloud cover. These cloud properties need to be harmonized. For this particular case the photolysis scheme's clouds agree better with observations than the aqueous chemistry scheme's clouds. Simulations using the photolysis scheme's clouds in the aqueous chemistry scheme result in more sulfur dioxide oxidizing to form sulfate aerosols due to more clouds present.

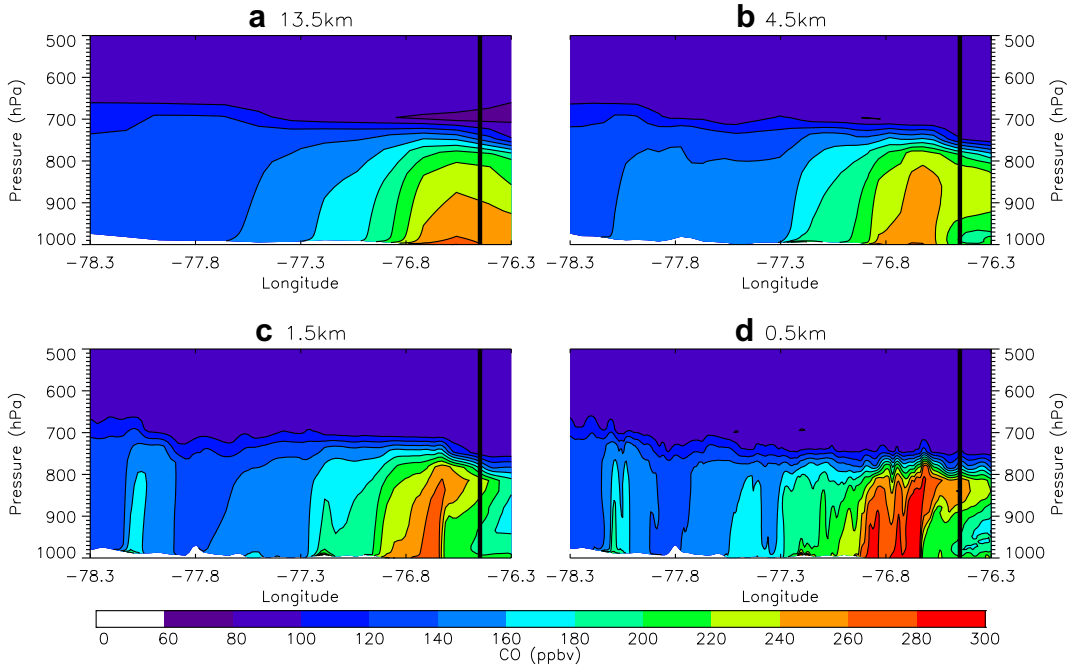

Fig. 13. West–east cross section of carbon monoxide (ppbv) passing between Washington, DC and Baltimore, MD at 39.1° latitude for the a) 13.5, b) 4.5, c) 1.5, and d) 0.5 km domains at 1900 UTC 9 July 2007. The coastline of the Chesapeake Bay is located at −76.42° longitude and is marked with a vertical black line. The local maximum in CO mixing ratio produced near the top of the boundary layer has been observed in aircraft profiles (Castellanos et al., in press; Taubman et al., 2006).

As resolution increases, more vigorous convective vertical mixing occurs in the PBL and between the PBL and free troposphere. Faster vertical mixing in the presence of fair-weather cumulus clouds results in more sulfur dioxide transport into clouds and more sulfate formation. More transport across the PBL to the free troposphere allows pollutants to have a longer lifetime and travel further downwind. The longer trace gases and aerosols remain in the atmosphere, the larger the radiative, microphysical, and climate impacts. Also, an increase in pollutant transport exacerbates air pollution downwind.

The bay breeze increases in strength as the resolution increases. The 13.5 km resolution simulation does not capture the bay breeze and allows ground-level pollutants to cross the coastline. This causes larger 8 h maximum ozone concentrations over the water and lower concentrations inland near the bay breeze convergence zone seen in finer resolution simulations and in observations. Even though ozone concentrations differ near the bay breeze convergence zone in the 4.5, 1.5, and 0.5 km simulations, a comparison of error statistics between model simulations and observations indicates that running CMAQ at a horizontal resolution of 4.5 km is sufficient for modeling ground-level ozone in the vicinity of the Chesapeake Bay. However, it should be noted that the 8 h maximum ozone concentrations near the convergence zone of the bay breeze on the western shore of the Chesapeake Bay, which is not co-located with an observational site, are sensitive to resolution equaling 93, 98, 101, and 107 ppbv for the 13.5, 4.5, 1.5, and 0.5 km simulations, respectively. Due to the sparseness of observational sites, it is difficult to prove that CMAQ simulations at resolutions greater than 4.5 km are more accurate at calculating ground-level ozone.

It is difficult to simulate or parameterize fine spatial scale features, such as fair-weather cumulus cloud development and a bay breeze, at a coarse resolution. However, it is impractical to run model simulations at a horizontal resolution of 0.5 km for many projects due to computational restraints. The results discussed earlier can be used to help improve coarse model simulations. Even though cloud fraction and liquid water content decreases with increasing resolution in the base case simulations, the rate of SO_2 oxidation increases with increasing resolution, due to more vertical transport through clouds. Also, more pollutants are transported out of the PBL to the free troposphere. These results suggest that the vertical diffusion scheme for coarse simulations could be modified to produce faster vertical transport to allow more pollutants to be transported into clouds and across the top of the boundary layer.

In order to simulate a bay, sea, or lake breeze at resolutions coarser than 4.5 km, a bay, sea, or lake breeze parameterization needs to be developed. Otherwise, finer horizontal resolutions are needed along coastlines. This can be accomplished with nested simulations along coastlines or a stretched grid with the resolution increasing as the distance from the coastline decreases.

5. Conclusions

In this study, CMAQ simulations at 13.5, 4.5, 1.5, and 0.5 km horizontal resolution are performed using the corresponding meteorological modeling results. Results show that more sulfur dioxide is converted to sulfate aerosols as the resolution increases when fair-weather cumulus clouds are present. Even though for the base case simulations there are fewer clouds in the higher resolution simulations, more pollutants are transported vertically through clouds causing more sulfur dioxide to be converted to sulfate aerosols. Also, in higher resolution simulations more pollutants are vented out of the PBL to the free troposphere, where winds are faster, and transported downwind at a faster rate.

CMAQ uses one method to diagnose clouds for aqueous chemistry calculations and another for photolysis rates. For this modeling scenario, use of the photolysis scheme's clouds in both the photolysis and aqueous chemistry schemes leads to better agreement with GOES visible satellite observations. Simulations using the photolysis scheme's clouds in the aqueous chemistry scheme displays an increase in sulfur dioxide oxidation due to the presence of more fair-weather cumulus clouds, showing the importance of accurately modeling the spatial coverage of fair-weather cumulus clouds in order to accurately model sulfate aerosol concentrations.

Our results indicate that higher resolution simulations are more capable of simulating horizontal temperature gradients that can cause a bay breeze to form and impact the transport of pollutants. The 4.5, 1.5, and 0.5 km WRF-UCM simulations produce a Chesapeake Bay breeze that starts sooner and is stronger throughout the day than the 13.5 km resolution simulations. This results in less pollutants being transported near the surface over the Chesapeake Bay and instead being transported aloft. Simulations at 4.5, 1.5, and 0.5 km resolution produce higher and more realistic 8 h maximum ozone concentrations at locations near the Bay Breeze convergence zone (e.g., Edgewood) and lower concentrations near the surface of the Chesapeake Bay.

Acknowledgements

This work was funded by NASA grant NNG066J046 and NASA Earth System Science Fellowship NNX06AF57H. Daewon Byun generously provided profound insight into the workings of CMAQ that helped make this research possible. Contributions from Dr. Jeff Stehr are gratefully acknowledged. Observations were supported by MDE.

References

Banta, R., Senff, C., Nielsen-Gammon, J., Darby, L., Ryerson, T., Alvarez, R., Sandberg, P., Williams, E., Trainer, M., 2005. A bad air day in Houston. Bulletin of the American Meteorological Society 86, 657–669. doi:10.1175/BAMS-86-5-657.

Boucouvala, D., Bornstein, R., 2003. Analysis and transport patterns during an SCOS97-NARSTO episode. Atmospheric Environment 37 (2), S73–S94.

Byun, D., Schere, K.L., 2006. Review of the governing equations, computational algorithms, and other components of the Models-3 Community Multiscale Air Quality (CMAQ) modeling system. Applied Mechanics Review 59, 51–77.

Byun, D.W., Pleim, J.E., Tang, R.T., Bourgeois, A., 1999. Meteorology-Chemistry Interface Processor (MCIP) for Models-3 community Multiscale Air Quality (CMAQ) Modeling System, EPA-600/R-99/030, pp. 12–21–12–90. Science Algorithms of the EPA Models-3 Community Multiscale Air Quality (CMAQ) Modeling System. U.S. Environmental Protection Agency, Washington, DC.

Castellanos, P., 2009. Analysis of Temporal Sensitivities and Vertical Mixing in CMAQ, and Measurements of NO_2 with Cavity Ring-down Spectroscopy, Ph.D. Thesis, Department of Chemical and Biomolecular Engineering, University of Maryland, College Park, MD, p. 165.

Castellanos, P., Marufu, L.T., Doddridge, B.G., Taubman, B.F., Schwab, J.J., Hains, J.C., Ehrman, S.H., Dickerson, R.R. Ozone, oxides of nitrogen and carbon monoxide during pollution events over the eastern US: an evaluation of emissions and vertical mixing. Journal of Geophysical Research (in press).

Chang, J.S., Brost, R.A., Isaksen, I.S.A., Madronich, S., Middleton, P., Stockwell, W.R., Walcek, C.J., 1987. A three-dimensional Eulerian acid deposition model: physical concepts and formulation. Journal of Geophysical Research 92, 14681–14700.

Chen, F., Dudhia, J., 2001. Coupling an advanced land–surface-hydrology model with the Penn State-NCAR MM5 modeling system. Part I: model implantation and sensitivity. Monthly Weather Review 129, 569–585.

Cohan, D.S., Hu, Y., Russell, A.G., 2006. Dependence of ozone sensitivity analysis on grid resolution. Atmospheric Environment 40, 126–135.

Colella, P., Woodward, P.R., 1984. The piecewise parabolic method (PPM) for gas-dynamical simulations. Journal of Computational Physics 54, 174–201.

Darby, L.S., 2005. Cluster analysis of surface winds in Houston, Texas, and the impact of wind patterns on ozone. Journal of Applied Meteorology 44, 1788–1806. doi:10.1175/JAM2320.1.

Daum, P.H., 1990. Observations of H_2O_2 and S(IV) in air, cloudwater, and precipitation and their implications for the reactive scavenging of SO_2. Atmospheric Research 25, 89–102.

Docker, D.W., Pope, C.A., Xu, X., Spengler, J.D., Ware, J.H., Fay, M.E., Ferris, B.G., Speizer, F.E., 1993. An association between air pollution and mortality in six U.S. cities. New England Journal of Medicine 329, 1753–1759.

Eatough, D.J., Arthur, R.J., Eatough, N.L., Hill, M.W., Mangelson, N.F., Richter, B.E., Hansen, L.D., 1984. Rapid conversion of $SO_2(g)$ to sulfate in a fog bank. Environmental Science and Technology 18, 855–869.

Emmons, L.K., Walters, S., Hess, P.G., Lamarque, J.-F., Pfister, G.G., Fillmore, D., Granier, C., Guenther, A., Kinnison, D., Laepple, T., Orlando, J., Tie, X., Tyndall, G., Wiedinmyer, C., Baughcum, S.L., Kloster, S., 2010. Description and evaluation of the model for ozone and related chemical tracers, version 4 (MOZART-4). Geoscientific Model Development 3, 43–67.

Evtyugina, M.G., Nunes, T., Pio, C., Costa, C.S., 2006. Photochemical pollution under sea breeze conditions, during summer, at the Portuguese West Coast. Atmospheric Environment 40, 6277–6293.

Eyth, A.M. and B. Brunk, 2005. New features in version 3 of the MIMS spatial Allocator, paper presented at 4th Annual CMAS Models-3 users' Conference, Chapel Hill, NC.

Finlayson-Pitts, B.J., Pitts, J.N., 2000. Chemistry of the Upper and Lower Atmosphere. Academic Press, San Diego, CA.

Gilliland, A.B., Hogrefe, C., Pinder, R.W., Godowitch, J.M., Foley, K.L., Rao, S.T., 2008. Dynamic evaluation of regional air quality models: assessing changes in O_3 stemming from changes in emissions and meteorology. Atmospheric Environment 42, 5110–5123.

Godowitch, J.M., Pouliot, G.A., Rao, S.T., 2010. Assessing multi-year changes in modeled and observed urban NOX concentrations from a dynamic model evaluation perspective. Atmospheric Environment 44, 2894–2901.

Grell, G.A., Devenyi, D., 2002. A generalized approach to parameterizing convection combining ensemble and data assimilation techniques. Geophysical Research Letters 29 Article 1693.

Hains, J.C., 2007. A Chemical Climatology of Lower Tropospheric Trace Gases and Aerosols over the Mid-Atlantic Region, Ph.D. Thesis, Department of Atmospheric and Oceanic Science, University of Maryland, College Park, MD, p. 254.

Hogrefe, C., Rao, S.T., Zurbenko, I.G., Porter, P.S., 2000. Interpreting the information in ozone observations and model predictions relevant to regulatory policies in the Eastern United States. Bulletin of the American Meteorological Society 81, 2083–2106.

Houyoux, M.R. and J. M. Vukovich, 1999. Updates to the Sparse Matrix Operator Kernel emissions (SMOKE) modeling system and Integration with Models-3, paper presented at the emission inventory: regional Strategies for the Future, Air and Waste Management Association, Raleigh, NC.

Jacob, D.J., Gottlieb, E.W., Prather, M.J., 1989. Chemistry of a polluted cloudy boundary layer. Journal of Geophysical Research 94, 12975–13002.

Janjic, Z.I., 1994. The step-mountain eta coordinate model: further developments of the convection, viscous sublayer and turbulence closure scheme. Monthly Weather Review 122, 927–945.

Jimenez, P., Jorba, O., Parra, R., Baldasano, J.M., 2006. Evaluation of MM5-EMICAT2000-CMAQ performance and sensitivity in complex terrain: high-resolution application to northeastern Iberian Peninsula. Atmospheric Environment 40, 5056–5072.

Klemp, J.B., Dudhia, J., Hassiotis, A., 2008. An upper gravity wave-absorbing layer for NWP applications. Monthly Weather Review 136, 3987–4004.

Kusaka, M., Kimura, F., 2004. Coupling a single-layer urban canopy model with a simple atmospheric model: impact on urban heat island simulation for an idealized case. Journal of the Meteorological Society of Japan 82, 67–80.

Kusaka, H., Kondo, H., Kikegawa, Y., Kimura, F., 2001. A simple single layer urban canopy model for atmospheric models: comparison with multi-layer and slab models. Boundary-Layer Meteorology 101, 258–329.

Lee, C., Martin, R.V., Donkelaar, A., Lee, H., Dickerson, R.R., Hains, J.C., Krotkov, N., Richter, A., Vinnikov, K., Schwabb, J.J., 2011. SO_2 emissions and lifetimes: estimates from inverse modeling using in situ and global, space-based (SCIAMACHI and OMI) observations, Journal of Geophysical Research 116, doi:10.1029/2010JD014758.

Lim, K.-S.S., Hong, S.-Y., 2010. Development of an effective double-moment cloud microphysics scheme with prognostic Cloud Condensation Nuclei (CCN) for weather and climate models. Monthly Weather Review 138, 1587–1612.

Mass, C., Ovens, D., Albright, M., Westrick, K., 2002. Does increasing horizontal resolution produce better forecasts?: the results of two years of real-time numerical weather prediction in the Pacific Northwest. Bulletin of the American Meteorological Society 83, 407–430.

Mudway, I.S., Kelly, F.J., 2000. Ozone and the lung: a sensitive issue. Molecular Aspects of Medicine 21, 1–48.

Mueller, S.F., Bailey, E.M., Cook, T.M., Mao, Q., 2006. Treatment of clouds and the associated response of atmospheric sulfur in the Community Multiscale Air Quality (CMAQ) modeling system. Atmospheric Environment 40, 6804–6820.

Odman, M.T., Hu, Y., 2009. Georgia Institute of Technology. Last accessed October 27, 2010. http://people.ce.gatech.edu/~todman/bugs/bugs.htm.

Otte, T., Pleim, J.E., 2010. The Meteorological-Chemistry Interface Processor (MCIP) for the CMAQ modeling system: updates through MCIPv3.4.1. Geoscientific Model Development 3, 243–256.

Pleim, J.E., 2007. A combined local and non-local closure model for the atmospheric boundary layer. Part 1: model description and testing. Journal of Applied Meteorology and Climatology 46, 1383–1395.

Pleim, J.E., Chang, J., 1992. A non-local closure model for vertical mixing in the convective boundary layer. Atmospheric Environment 26A, 965–981.

Samet, J.M., Dominici, F., Curriero, F.C., Coursac, I., Zeger, S.L., 2000. Fine particulate air pollution and mortality in 20 U.S. cities, 1987–1994. New England Journal of Medicine 343, 1742–1749.

Shine, K.P., 2000. Radiative forcing of climate change. Space Science Reviews 94, 363–373.

Shou, Y., Zhang, D.-L., 2010. Impact of environmental flows on the urban daytime boundary layer structures over the Baltimore metropolitan region. Atmospheric Science Letters 11, 1–6.

Skamarock, W.C., Klemp, J.B., Dudhia, J., Gill, D.O., Barker, D.L., Duda, M.G., Huang, X.-Y., Wang, W., Powers, J.G., 2008. A Description of the Advanced Research WRF Version 3, NCAR Technical Note, NCAR/TN-475+STR. NCAR, Boulder, CO.

Sokhi, R.S., San Jose, R., Kitwiroon, N., Fragkou, E., Perez, J.L., Middleton, D.R., 2006. Prediction of ozone levels in London using the MM5-CMAQ modelling system. Environmental Modelling and Software 21, 566–576.

Taubman, B.F., Hains, J.C., Thompson, A.M. , Marufu, L.T., Doddridge, B.G., Stehr, J.W., Piety, C.A., Dickerson, R.R., 2006. Aircraft vertical profiles of trace gas and aerosol pollution over the mid-Atlantic United States: Statistics and meteorological cluster analysis, Journal of Geophysical Research 111, D10S07, doi:10.1029/2005JD006196.

U.S. Environmental Protection Agency, 2003. User's Guide to MOBILE6.1 and MOBILE6.2: Mobile Source Emission Factor Model, EPA420-R-03-010. U.S. EPA National Vehicle and Fuel Emissions Laboratory, Ann Arbor, MI, p. 262.

Vukovich, J. and T. Pierce, 2002. The Implementation of BEIS-3 within the SMOKE modeling framework, Presented at emissions Inventories – Partnering for the Future, paper presented at the 11th emissions inventory Conference of the U.S. Environmental Protection Agency, Research Triangle Park, NC.

Weijers, E.P., Khlystov, A.Y., Kos, G.P.A., Erisman, J.W., 2004. Variability of particulate matter concentrations along roads and motorways determined by a moving measurement unit. Atmospheric Environment 38, 2993–3002.

Yarwood, G., Rao, S., Yocke, M., Whitten, G.Z., 2005. Updates to the Carbon Bond Mechanism: CB05, RT-0400675. U.S. Environmental Prediction Agency, Washington, DC.

Yegorova, E.A., D.J. Allen, C.P. Loughner, K.E. Pickering, and R.R. Dickersion, in press. Characterization of an eastern U.S. severe air pollution episode using WRF/chem., Journal of Geophysical Research.

Yu, S., Mathur, R., Sarwar, G., Kang, D., Tong, D., Pouliot, G., Pleim, J., 2010. Eta-CMAQ air quality forecasts of O_3 and related species using three different photochemical mechanisms (CB4, CB05, SAPRC-99): comparisons with measurements during the 2004 ICARTT study. Atmospheric Chemistry and Physics 10, 3001–3025.

Yu, S., Mathur, R., Schere, K., Kang, D., Pleim, J., Otte, T.L., 2007. A detailed evaluation of the Eta-CMAQ forecast model performance for O_3, its related precursors, and meteorological parameters during the 2004 ICARTT study. Journal of Geophysical Research 112, D12S14. doi:10.1029/2006JD007715.

Zhang, D.-L., Chang, H.-R., Seaman, N.L., Warner, T.T., Fritsch, J.M., 1986. A two-way interactive nesting procedure with variable terrain resolution. Monthly Weather Review 114, 1330–1339.

Zhang, D.-L., Shou, Y., Dickerson, R.R., 2009. Upstream urbanization exacerbates urban heat island effects. Geophysical Research Letters 36, L241–L244. doi:10.1029/2009GL041082.